Measurement of the Spatial Distribution of Birefringence in Optical Fibers

Marc Wuilpart, *Student Member, IEEE*, Patrice Mégret, *Member, IEEE*, Michel Blondel, Alan J. Rogers, *Senior Member, IEEE*, and Yves Defosse

***Abstract*—In this letter, we describe a technique for the measurement of the birefringence spatial distribution in a single-mode optical fiber with a resolution of 1 m. This technique is based on a polarization optical time-domain reflectometer using a rotary linear polarizer. We report results performed on different types of fibers: standard step-index and dispersion shifted fibers.**

***Index Terms*—Beat length, birefringence, distributed measurement, polarization mode dispersion, polarization optical time-domain reflectometer.**

I. Introduction

The use of dispersion-shifted optical fibers (DSF), and dispersion compensating fibers (DCF) have minimized the effect of chromatic dispersion on the bandwidth of an optical link. Polarization mode dispersion (PMD) has therefore become the most serious limiting factor in high-speed optical communication systems. The PMD of a fiber depends on two parameters: the mean beat length (L_B) and the mean coupling length (L_C) [1], [3]. The beat length is related to the birefringence, defined as the phase delay difference between the two principal states. The mean coupling length is related to the polarization mode coupling characterizing, a standard telecommunication fiber [3]. There exists several polarization-optical time-domain reflectometer (POTDR)-based techniques for distributed birefringence measurement [2] but, as far as we know, they only allow the determinination of the mean birefringence on several hundreds of meters. In this letter, we describe a technique for measuring the spatial distribution of the birefringence in a single-mode optical fiber, with a resolution of 1 m.

II. Theory

In general, an optical fiber with axially varying birefringence can be represented by a series of concatenated homogeneous elements, each characterized by a Jones matrix, as illustrated in Fig. 1(a). Moreover, we suppose that the fiber only exhibits linear birefringence, as it is usually accepted in telecommunication fibers. Let us consider a double passage, forward and then backward, of the light into the fiber. The resultant birefringence for light propagating forward to the end of the ith element and then backward to the launch end is given by the successive products of the relevant matrices [4]

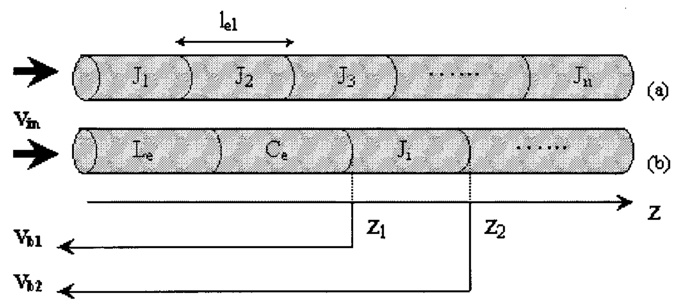

Fig. 1. (a) Fiber Modeling: J_i is the Jones matrix of the ith element. (b) Equivalent linear retarder/rotator pair. L_e and C_e are the Jones matrix of the linear retarder and the rotator, respectively.

$$J_{Bi} = (J_i J_{i-1} \cdots J_2 J_1)^T (J_i J_{i-1} \cdots J_2 J_1) \tag{1}$$

where J_i^T is the transpose of J_i. Let us now consider that we want to measure the birefringence β_i of the ith element. The concatenation of the preceding sections (1 to $i-1$) can be modeled as a series combination of a pure linear retarder described by a Jones matrix L_e, and a pure rotator described by a Jones matrix C_e, as illustrated in Fig. 1(b).

It can than be shown [5] that the roundtrip Jones matrices described in (1) are equivalent to a linear retarder and may be written by the following general form:

$$J_{Bi} = \begin{pmatrix} A_i + jB_i & jC_i \\ jC_i & A_i - jB_i \end{pmatrix} \tag{2}$$

with

$$A_i^2 + B_i^2 + C_i^2 = 1. \tag{3}$$

If the Jones vectors $\mathbf{V}_{\mathrm{b1}}$ and $\mathbf{V}_{\mathrm{b2}}$, resulting from the light propagating forward to z_1 and z_2, respectively, and then propagating backward to the launch end [see Fig. 1(b)], are measured, J_{Bi} and J_{Bi-1} can be deduced if the input state $\mathbf{V}_{\mathbf{in}}$ is known. J_{Bi} and J_{Bi-1} are the roundtrip Jones matrices resulting from backscattering at the end of the ith and the $(i-1)$th element, respectively. The product matrix $C_e^{-1} J_i^2 C_e$ can then be calculated [5]. This matrix may be written in the Jones formalism by [5]

$$C_e^{-1} J_i^2 C_e = \begin{pmatrix} A + jB & jC \\ jC & A - jB \end{pmatrix} \tag{4}$$

Manuscript received April 6, 2001; revised May 4, 2001. The work of M. Wuilpart was supported by the Fonds pour la Formation à la Recherche dans l'Industrie et dans l'Agriculture, Belgium. The work of P. Mégret was supported by the Inter-University Attraction Pole Program of the Belgian Government.

M. Wuilpart, P. Mégret, and M. Blondel are with the Faculté Polytechnique de Mons, Service d'Electromagnétisme et de Télécommunications, B-7000 Mons, Belgium (e-mail: wuilpart@telecom.fpms.ac.be).

A. J. Rogers is with the Department of Electronic and Electrical Engineering, King's College London, WC2R 2LS Strand, U.K.

Y. Defosse is with Multitel a.s.b.l., B-7000 Mons, Belgium.

Publisher Item Identifier S 1041-1135(01)06413-8.

where $A = \cos(\beta_i l_{el})$, l_{el} is the element length, and β_i is the local birefringence i.e., the phase delay difference between the two local linear principal states. Hence, it appears that β_i can be determined after measuring $\mathbf{V}_{b1}$ and $\mathbf{V}_{b2}$ if we assume β_i is between 0 and $\pi/2$. This last condition supposes that the local beat length is bigger than 4 m for a measurement resolution length of 1 m, which is usually the case for a telecommunication fiber. Measuring the distributed birefringence, therefore, consists to determine the A_i, B_i, and C_i parameters related to the different roundtrip Jones matrices described in (1).

III. Principle of Measurement

Because it is not convenient to measure a Jones vector, the use of the Stokes formalism, which describes a state of polarization in terms of measurable optical powers, is more suitable. It is why we will use this formalism for the following of this letter. The polarization properties of an optical device are then described by a four-by-four Mueller matrix. The corresponding Mueller matrix of (2) may be written

$$M_{B_i} = \begin{pmatrix} 1 & 0 & 0 & 0 \\ 0 & A_i^2+B_i^2-C_i^2 & 2B_iC_i & -2A_iC_i \\ 0 & 2B_iC_i & A_i^2+C_i^2-B_i^2 & 2A_iB_i \\ 0 & 2A_iC_i & -2A_iB_i & A_i^2-B_i^2-C_i^2 \end{pmatrix}. \quad (5)$$

If we want to measure $\mathbf{V}_{b1}$ and $\mathbf{V}_{b2}$ for each element, we need to measure the complete polarization state evolution of the backscattered light, which is quite difficult to implement. An easier setup has therefore been developed. It is similar to a POTDR setup, but it uses a rotary polarizer at the fiber input, which is also used as the backscattered signal analyzer. Let us consider the polarizer/analyzer imposing a 0° linear input state of polarization with respect to an arbitrary Ox axis. The first component, representing the optical powers, of the normalized Stokes vector resulting from the light passing through the polarizer, propagating forward to the end of the ith element, and then backward to the launch end, and finally passing through the analyzer is given by

$$P_0 = A_i^2 + B_i^2. \quad (6)$$

In the same way, when the polarizer/analyzer imposes input linear states of 45° and 22.5°, the detected powers are, respectively,

$$P_{45} = A_i^2 + C_i^2 \quad (7)$$

$$P_{22.5} = B_iC_i + \frac{1 + A_i^2}{2}. \quad (8)$$

From (3), (6)–(8), it appears that the measurement of the backscattered field evolution for three different positions of the polarizer/analyzer enables to determine the A_i^2, B_i^2, C_i^2, and B_iC_i values related to the different round-trip matrices described in (1). The sign ambiguities on A_i, B_i, and C_i lead to two different possible solutions for each β_i. The value of β_i can then be determined by supposing that two successive β_i are close to each other.

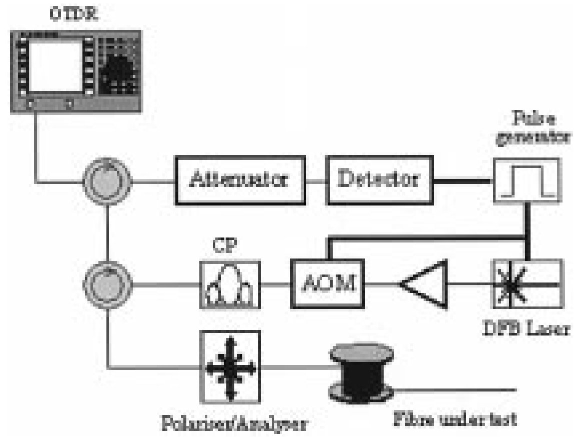

Fig. 2. Experimental setup. The OTDR pulses modulates a 1550-nm DFB laser via a pulse generator. After amplification, the pulses are continuously Rayleigh-backscattered as they propagate down the fiber, and the emerging backscattered light is directed by the circulators onto the OTDR detector. An AOM is used to suppress the ASE of the EDFA between two successive pulses.

The experimental setup is shown in Fig. 2. Since the coherence of a commercial OTDR source is weak, the pulses cannot directly be sent into the fiber for this application and a highly coherent source has to be used. The spectral width of the laser source in the measurement system has to be sufficiently narrow to avoid depolarization of the light for the whole fiber length under test. The OTDR pulses, therefore modulates a 1550-nm DFB laser via a pulse generator. The pulse width was set to 10 ns in order to obtain a spatial resolution of 1 m. The coherence noise due to the high coherence of the source is reduced by performing the measurement, while the laser drifts in wavelength. Further reduction of this noise can be numerically done by using the relationship between (6)–(8). The power level of this laser being 0 dBm, an erbium-doped fiber amplifier (EDFA) is used to obtain sufficient pulse peak power into the fiber. An acoustooptical modulator (AOM) then suppresses the amplified spontaneous noise of the EDFA between two successive pulses. The rotary-linear polarizer is placed at the fiber input, and a polarization controller (CP) is used to obtain the maximum power after the polarizer. Light pulses are continuously Rayleigh backscattered as the pulse propagates down the fiber, and the emerging backscattered light is directed by the circulators onto the OTDR detector. Three POTDR traces corresponding to a polarizer angle of 0°, 45°, and 22.5°, respectively, are then recorded and analyzed by a computer, which calculates the distributed birefringence.

IV. Results and Discussion

The computed spatial birefringence distributions related to a standard SI, and DSFs that have been performed by using the technique described in Section III and are shown in Fig. 3(a) and (b), respectively. These fibers were spooled on a drum, which had a diameter of 200 mm. In order to compare this measurement process with the level crossing rate (LCR) technique

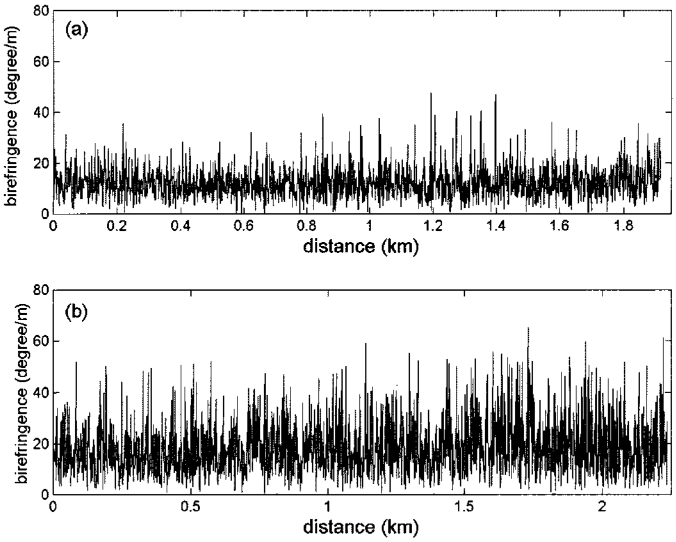

Fig. 3. Birefringence spatial distribution of (a) an SI optical fiber and (b) DSF. The DSF presents higher local birefringence values than the conventional SI fiber. This may be explained by the higher doping concentrations, and more complex index profiles of these fibers, which introduce higher internal stresses.

TABLE I
BEAT LENGTH VALUES OBTAINED BY OUR METHOD AND BY THE LCR TECHNIQUE DESCRIBED IN [2]

Fibers	L_B (m)	
	$2\pi/\langle\beta_i\rangle$	LCR
SI Fiber	29.6	26.7
DSF	19.2	19.1

[2], which allows the measurement of the mean beat length L_B along the fiber, we computed L_B from our results by means of $L_B = 2\pi/\langle\beta_i\rangle$, where $\langle\beta_i\rangle$ is the mean birefringence value along the fiber.

The results are summarized in Table I. A good agreement is observed between the two methods, which confirms the validity of the technique described in this letter. We observe that the DSF presents higher local birefringence values than the conventional an SI fiber. This may be explained by the higher doping concentrations and the more complex index profiles of this fiber, which introduce higher internal stresses [2]. In Fig. 4(a) and (b), we show the histograms of β_i obtained from our measurements. The black curves represent the data fit by a Rayleigh distribution. It appears that the PDF of the birefringence along the fiber length is close to a Rayleigh distribution, which agrees with the model adopted in [2].

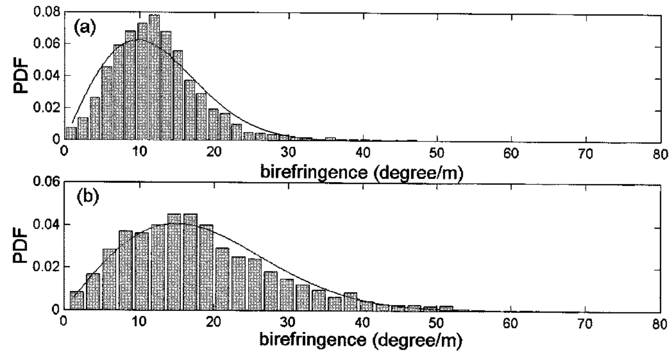

Fig. 4. (a) Histogram of the SI fiber local birefringence. (b) Histogram of the DSF local birefringence. The black curves represent the data fit by a Rayleigh distribution. The birefringence statistical distribution along the fiber length is then close to a Rayleigh distribution, which agrees with the model adopted in [2].

V. CONCLUSION

In this letter, we described a new POTDR trace analysis, which enables the computation of the birefringence spatial distribution in a single-mode optical fiber with 1-m resolution. The experimental setup is based on a POTDR using a rotary linear polarizer, which is quite simple to implement. We showed that the measurement of three POTDR traces enables to determine the distributed birefringence. A good agreement is observed between this technique and the LCR technique, and we experimentally verified the Rayleigh distribution of the birefringence along the fiber. The measurement applied on a SI fiber and a DSF showed that the birefringence is bigger for the second fiber, which is due to the presence of higher stresses in this fiber type.

ACKNOWLEDGMENT

The authors are very grateful to Multitel a.s.b.l. for fruitful discussions and technical help.

REFERENCES

[1] N. Gisin, J. P. Von der Weid, and J. P. Pellaux, "Polarization mode dispersion of short and long single-mode fibers," *J. Lightwave Technol.*, vol. 9, pp. 821–827, July 1991.

[2] F. Corsi, A. Galtarossa, and L. Palmieri, "Beat length characterization based on backscattering analysis in randomly perturbed single-mode fibers," *J. Lightwave Technol.*, vol. 17, pp. 1172–1178, July 1999.

[3] B. Huttner, B. Gisin, and N. Gisin, "Distributed PMD measurement with a polarization-OTDR in optical fibers," *J. Lightwave Technol.*, vol. 17, pp. 1843–1848, Oct. 1999.

[4] A. J. Rogers, Y. R. Zhou, and V. A. Handerek, "Computational polarization-optical time domain reflectometry for measurement of the spatial distribution of PMD in optical fibers," in *Proc. OFMC*, 1997, pp. 126–129.

[5] M. Wuilpart, A. J. Rogers, P. Mégret, and M. Blondel, "Fully-distributed polarization properties of an optical fiber using the backscattering technique," in *Proc. ICAPT, SPIE*, vol. 4087, 2000.